

THERMAL DAMAGE DUE TO INCIDENTAL CONTINUOUS CO₂ LASER IRRADIATION ON HUMAN SKIN

by

Khalid S. SHIBIB

Department of Laser and Optoelectronics Engineering, University of Technology, Baghdad, Iraq

Original scientific paper
UDC: 621.375.826:612.795
DOI: 10.2298/TSCI1002451S

The use of laser instruments in almost every aspect of technology may lead to sudden exposing of human skin to laser radiation, especially with an invisible laser, such as continuous CO₂ laser, causing harmful thermal damage to the exposed area. This phenomena is studied in this work where the size of thermal damage is obtained using a well-known thermal dose equation which requires the transient temperature distributions obtained from finite element solution of the axi-symmetric heat equation. In this work a numerical simulation of these processes is applied indicating that the size of thermal damage zone inside human tissue seems to increase as power increases even if the exposing time is reduced, whereas the shape of thermally damage zone extends laterally much more than in-depth due to the effect of absorption coefficient and perfusion rate of skin tissue. Finally, this work may establish the concept of numerical investigation of an incidental laser hazard on human skin.

Key words: *finite element method, thermal skin damage, CO₂ laser, bioheat equation*

Introduction

Due to large increase of laser systems application in different field of science, such as medicine, industry, and measurements [1], an incidental exposing of laser radiation on human skin may occur, causing a rapid damage to human skin combining with pain, especially with high laser power. This work focuses on the influence of different power of continuous CO₂ laser radiation to show its effect on pain and damage of human skin. An axi-symmetrical bioheat equation with laser beam interacting with the tissue at the skin surface and a boundary condition of convection combined with internal perfusion rate has been solved numerically to determine temperature distribution through human tissue, from which the thermal dose equation is used to determine the necroses zone.

Simulation procedure and theory

Simulation procedure

As the continuous CO₂ laser hit the skin the main part of it will transform into heat which will transfer across the tissue, leading to rapid increase in skin temperature. As it reaches

* e-mail: assprofkh@coolgoose.com

44 °C , which is known to be the threshold limit of pain, a nervous system may respond with a speed of 100 m/s, [2], taking for a 0.5 m from the center of nervous system 0.01 s to react. Thus, the human will move away from the source of pain with a delay of at least 0.01 s. The thermal damage at the time of pain sensation plus time of response should be calculated using a well known thermal dose equation depending on the transient temperature distribution obtained from the finite element solution of axi-symmetric heat equation. Also the thermal damage corresponding to the temperature higher than 42 °C is calculated to obtain the total damage zone due to incidental laser radiation.

Partial differential equation and boundary conditions

Based on the well known Pennes bioheat equation [3], using symmetrical nature of the problem, the axi-symmetric bioheat equation is applied:

$$\rho c \frac{\partial T}{\partial t} + \frac{1}{r} k_r \frac{\partial}{\partial r} \left(r \frac{\partial T}{\partial r} \right) + k_z \frac{\partial^2 T}{\partial z^2} = Wc_b (T_B - T) + \dot{Q} + \dot{Q}_m \quad (1)$$

Only one-half of the cross-section is considered because of symmetry, as shown in fig. 1. The basal temperature is assumed to be 37 °C, the heat generation is produced by the interaction of laser photons with tissue, the convective heat transfer is assumed to be 25 W/m²K, the environmental temperature 26 °C, the density of blood 1060 kg/m³, and its specific heat 3770 J/kgK [4]. The metabolic rate of tissue \dot{Q}_m is assumed to be 1 W/kg for skin, 0.32 W/kg for fat, and 0.67 W/kg for muscle [5]. The thermal properties and perfusion rate of different layers of skin are illustrated in tab. 1 and the temperature at threshold pain limit is assumed to be 44 °C [1].

Laser as heat source

The usual pattern of laser beam is that of Gaussian distribution with the irradiation distribution through its radius [6]:

$$I = I_{\max} \exp \left(-\frac{2r^2}{w_0^2} \right) \quad (2)$$

where

$$I_{\max} = \frac{2p}{\pi w_0^2} \quad (2a)$$

As laser interacts with the tissue the intensity of light at any depth can be written as, [1]:

$$q_z = (1 - RF)I \exp(-\mu z) \quad (3)$$

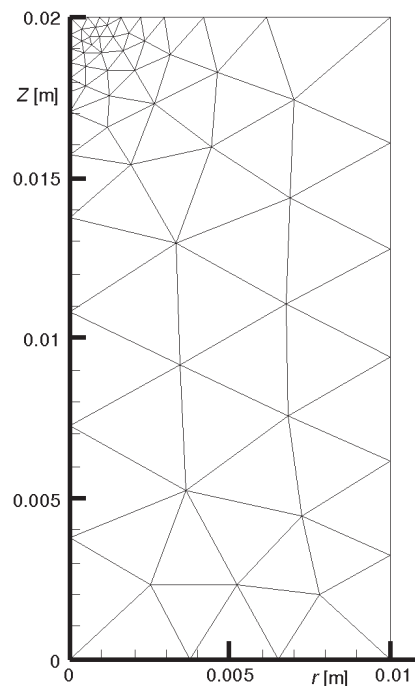


Figure 1. Mesh and dimensions of a selected domain

Table 1. Thermal properties of different kinds of human tissue [3, 16]

Tissue	ρ [kgm ⁻³]	c [Jkg ⁻¹ K ⁻¹]	k [Wm ⁻¹ K ⁻¹]	W_0 [kgs ⁻¹ m ⁻³]	Thickness [μ m]
Epidermis	1200	3590	0.23	0.0	80
Dermis	1200	3300	0.45	1.35	2000
Subcutaneous tissue	1000	2675	0.19	1.35	18000

where RF is the reflectivity, being for CO₂ laser on human skin approximately equal to zero, and μ – the absorption coefficient which is equal to 594 per cm for the native skin [7]. Now, the heat generation at any depth is:

$$\dot{Q}(r, z) = \frac{dq_z}{dz} = I\mu \exp(-\mu z) \quad (4)$$

Finite element formulation

The space-wise discretization of axi-symmetric heat equation subjected to the above boundary conditions can be accomplished using Galerkin method. The volume of interest, Ω , is divided into a number of elements, Ω^e , with the usual shape function N_i associated with each node, so that the unknown function T is approximated through the solution domain at any time by:

$$T = \sum N_i(r, z, t) T_i(t) \quad (5)$$

where $T_i(t)$ are the nodal temperatures. Substitution of the above equation into bioheat equation and the application of Galerkin method results into a system of ordinary differential equations of the form [8]:

$$[C]\dot{\bar{T}} + [K]\bar{T} = [\bar{F}] \quad (6)$$

where $\bar{T} = \begin{bmatrix} \frac{\partial T_1}{\partial t} \\ \frac{\partial T_2}{\partial t} \\ \dots \\ \frac{\partial T_p}{\partial t} \end{bmatrix}$, $\bar{T} = \begin{bmatrix} T_1 \\ T_2 \\ \dots \\ T_p \end{bmatrix}$, and $[\bar{F}] = \begin{bmatrix} F_1 \\ F_2 \\ \dots \\ F_p \end{bmatrix}$ and p is the total numbers of nodes.

The typical matrix elements are:

$$K_{ij} = \int_{\Omega^e} k_r \frac{\partial N_i}{\partial r} \frac{\partial N_j}{\partial r} + k_z \frac{\partial N_i}{\partial z} \frac{\partial N_j}{\partial z} d\Omega + \int_{\Gamma^e} (N_i W c_b) d\Omega + \int_{\Gamma^e} N_i h d\Gamma \quad (7)$$

$$C_{ij} = \int_{\Omega^e} \rho c N_i N_j d\Omega \quad (8)$$

$$F_i = \int_{\Gamma^e} N_i (Q - hT_\infty) d\Gamma = \int_{\Omega^e} N_i (\dot{Q} - Q_m + Wc_b T_B) d\Omega \quad (9)$$

where K_{ij} , C_{ij} , and F_i indicate the contribution of each element in the global matrices [K], [C], and [F], respectively.

In the above, the summation are taken over the contribution of each element, Ω^e , in the element volume and Γ^e refers only to the element with external boundary on which surface condition is applied. To avoid iteration at each time step, the unconditionally stable three level scheme is applied here, proposed by Lees [8], using the shape function which normalizes to time interval, and applying the weighted residual theory to eq. (6), resulting in the matrix form:

$$\frac{3[C_n]}{2\Delta t} [K_n] \bar{T}_{n-1} - [K_n] \bar{T}_n + [K_n] \bar{T}_{n+1} = \frac{3}{2\Delta t} [C_n] \bar{T}_{n-1} + 3\bar{F} \quad (10)$$

In this solution a well-known method suggested by Comini, [8], is used to avoid iteration with each time step. The values of matrices at the intermediate time will be sufficient to solve the simultaneous equations at each time step. The values of the temperature at the end of the total three level will be replaced by the intermediate values for the next time step and so on, whereas two starting values of the temperature distribution can be assumed to start the solution of eq. (10). It is to be noted that some experience is necessary while meshing the region of interest since small elements are required near the surface where laser interacts with tissue, as shown in fig. 1. Also a self adjusting time step can be used to reduce running time.

Thermal dose calculations

The thermal dose calculation in term of equivalent minutes at 43 °C is used to estimate the necroses tissue volume, and is calculated using the following equation [9-14]:

$$TD = \int_{t_0}^{t_f} S^{(T-43)} dt \quad (11)$$

where $S=2$ for $T = 43$ °C and $S=4$ for 37 °C $< T < 43$ °C. The thermal dose value required for the total necrosis ranges from 25 to 240 minutes for brain to muscle tissues [13, 14], the latter taken in this work as the necrosis limit. The thermal dose is calculated during the period of effective temperature exposure (*i. e.* as long as temperature is greater than 42 °C). The thermal dose is calculated throughout the solution and any elements will be shown to exceed the limit of necrosis as the value of thermal dose exceeded the limit of 240 minutes.

Thermal properties of tissue and perfusion rate

Many references have well established the thermal properties of human tissue which are used in this work, tab. 1. Having in mind a decrease in perfusion at temperatures over 45 °C, resulting from heat-induced damage to blood capillaries [15], the value of perfusion rate at any location and time can be obtained using Arrhenius damage integral [16]:

$$\Psi(r, z, t) = \int_{t_0}^t A_{\text{freq}} \exp \left(-\frac{E_a}{RT(t)} \right) dt \quad (12)$$

where A_{freq} and E_a are presented for blood flow collapse (*i. e.* $A_{\text{freq}} = 1.98 \cdot 10^{-6}$ per second, and $E_a = 6.67 \cdot 10^5$ J/mol [16]). The perfusion rate was calculated continuously during the treatment as [16]:

$$W(r, z, t) = W_0[1 - \exp(-\Psi)] \quad (13)$$

Results and discussion

The initial temperature distribution through tissue can be obtained using the solution procedure described. If no laser radiation is taken into account, the resulting temperature distribution is shown in fig 2, obtained assuming an initial temperature throughout the tissue of 37 °C. This steady-state condition can be reached after 310 s from the imposing convection heat transfer at the skin surface and only metabolic heat generation with perfusion coefficient applied inside the tissue. This may verify the accuracy of the numerical simulation where the temperature of the skin surface is usually 33.5 °C.

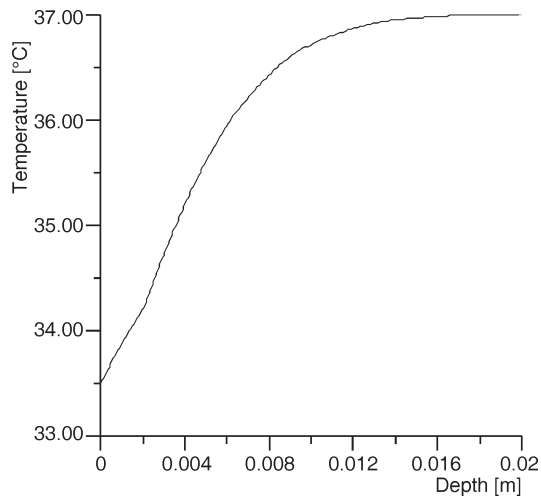


Figure 2. Initial temperature distribution across human body starting from epidermis

The simulation is carried out for laser spot diameter of 1 mm and the laser power with Gaussian distribution varying from 1 to 2000 W, to show influence on necrosis depth and time of heat relief (*i. e.* time to reach temperature less than 42 °C after exposing to laser radiation). No damage occurs for laser power of 1~100 W, for laser power of 500 W the maximum effected depth is 0.55 mm, for laser power of 1000 W it is 0.6 mm, and for laser power of 2000 W it is 0.9 mm, as shown in fig. 3 and tab. 2.

Table 2. Depth of necroses zone, heat relief and sensation time vs. laser power

Laser power [W]	Sensation time of pain [s]	Heat relief time [s]	Depth of necroses zone [mm]
100	0.001	0.778	0
500	0.0008	1.9875	0.55
1000	0.0004	2.01	0.6
2000	0.0002	4.7925	0.9

The shape of necroses zone is extending in lateral direction due to high absorption coefficient of tissue, zero perfusion coefficient in epidermis and high perfusion coefficient in the adjusting layer, even if it may collapse at the elevated temperature. As an example the tempera-

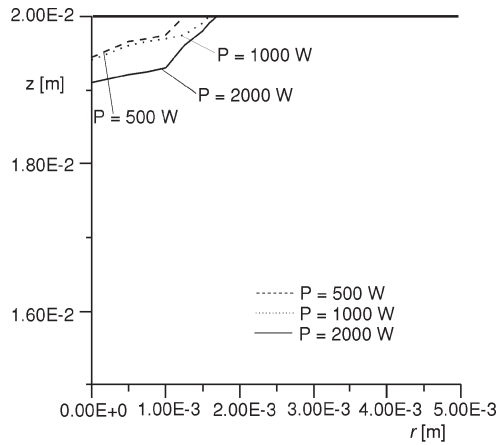


Figure 3. Enlarge view of necroses zone at various level of laser power

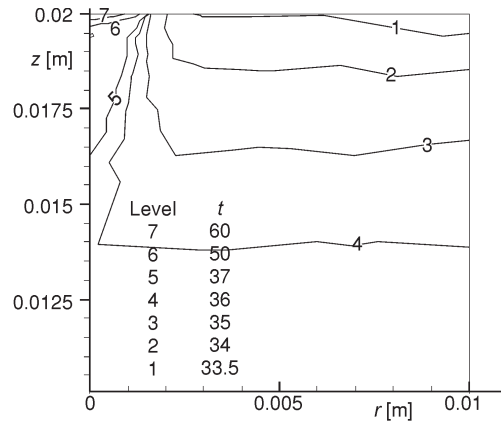


Figure 4. Temperature distributions at the cutoff time (0.0108 s) for laser power 500 W

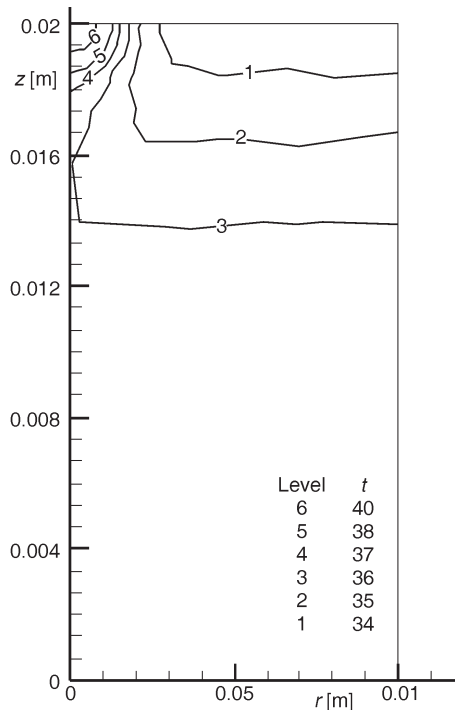


Figure 5. Temperature distribution at heat relief time (1.9875 s) for laser power of 500 W

ture distribution for laser power of 500 W at the cutoff time (sum of sensation and response time) and the heat relief time is shown in figs. 4 and 5, respectively. The delay in response which is equal to 0.01 s will lead to increase in skin temperature which may lead to irreversible damage in the skin layers for the laser power greater than 100 W. The increased perfusion rate seems to decrease the depth of necroses zone and since the upper part of skin has zero perfusion rates then the lateral extension of necroses zone in this region is logical.

Conclusions

The finite element method has been used successfully to solve the bioheat equation in order to get temperature distribution through tissue, from which the necroses zone due to incidental continuous CO₂ laser radiation is determined.

From the result of this work it is shown that as laser power is increased the size of thermal damage zone is increased as well, although the exposed time is slightly shorter. The damage zone extends laterally more than in-depth due to

high absorption coefficient of tissue, whereas perfusion coefficient is zero at epidermis and has relatively large value in the in-depth skin layers. Based on this work one may establish the limit of damage that occurs due to incidental laser irradiation.

Nomenclature

A_{freq}	– frequency factor, [s ⁻¹]
c	– specific heat, [Jkg ⁻¹ K ⁻¹]
E_a	– activation energy, [Jmol ⁻¹]
h	– convective heat transfer coefficient, [Wm ⁻² K ⁻¹]
I	– power intensity, [Wm ⁻²]
k	– thermal conductivity, [Wm ⁻¹ K ⁻¹]
N	– shape function
p	– power, [W]
Q	– heat flux, [Wm ⁻²]
\dot{Q}	– heat generation per unit volume, [Wm ⁻³]
Q_m	– metabolic heat generation per unit volume, [Wm ⁻³]
q	– light intensity, [Wm ⁻²]
RF	– reflectivity
r	– radial dimension, [m]
S	– constant
T	– temperature, [°C]
TD	– thermal dose, [minutes]
t	– time, [s]
W	– perfusion rate, [kgs ⁻¹ m ⁻³]
w_0	– radius of laser beam, [mm]
z	– longitudinal dimension, [m]
[C], [K], [F]	– global matrices

Greek letters

Γ	– surface of interest, [m ²]
μ	– absorption coefficient, [cm ⁻¹]
ρ	– density, [kgm ⁻³]
Ψ	– Arrhenius damage integral
Ω	– volume of interest, [m ³]

Subscripts

B	– basal
b	– blood
f	– final
m	– metabolic
max	– maximum
o	– initial
p	– total number of nodes
r	– radial axis symmetry dimension
z	– longitudinal axis symmetry dimension
$n-1, n,$	
$n+1$	– time steps
∞	– environmental

References

- [1] Hamed, M., Nadeau, V., Dickinson, M. R., A Novel Modeling and Experimental Technique to Predict and Measure Tissue Temperature during CO₂ Laser Stimuli for Human Pain Studies, *J. Lasers Med. Sci.*, 21 (2006), 2, pp. 95-100
- [2] Kraus, D., Concept in Modern Biology, Globe Book Company, New York, USA, 1969
- [3] Pennes, H. H., Analysis of Tissue and Arterial Blood Temperatures in the Resting Human Forearm, *Journal of Applied Physiology*, 1 (1948), 2, pp. 93-122
- [4] Torvi, D. A., Dale, J. D., Finite Element Model of Skin Subjected to a Flash Fire, *ASME J. Bio-mech. Eng.*, 116 (1994), 3, pp. 250-255
- [5] Murat, T., et al., The Bio-Heat Transfer Equation and its Application in Hyperthermia Treatments, *Engineering Computations International Journal for Computer-Aided Engineering and Software*, 23 (2006), 4, pp. 451-453
- [6] Majumdar, N. C., Kochhar, V. K., Thermal Effect of Pulsed Laser on Human Skin, *Def Sci. J.*, 35 (1985), 1, pp. 25-32
- [7] Choi, B., et al., Thermo Graphic and Histological Evaluation of Laser Skin Resurfacing Scans, *IEEE Journal of Selected Topics in Quantum Electronics*, 5 (1999), 4, pp. 1116-1125
- [8] Lewis, R.W., et al., The Finite Element Method, in: Heat Transfer Analysis, John Wiley and Sons Ltd., Chichester, U. K., 1996
- [9] Sapareto, S. A., Dewey, W. C., Thermal Dose Determination in Cancer Therapy, *Int. J. Radiat. Oncol. Biol. Phys.*, 10 (1984), 6, pp. 787-800
- [10] Chato, J. C., Fundamentals of Bioheat Transfer, in: Thermal Dosimetry Planning, Springer-Verlag, Berlin, 1990
- [11] Roemer, R. B., Thermal Dosimetry, in: Thermal Dosimetry Planning, Springer-Verlag, Berlin, 1990
- [12] Arkin, H., Xu, X., Holmes, K. R., Recent Developments in Modeling Heat Transfer in Blood Perfusion Tissues, *IEEE Trans. Biomed. Eng.*, 41 (1994), 2, pp. 97-107

- [13] Dewey, W. C., Arrhenius Relationships from the Molecules and Cell to the Clinic, *Int. J. Hyperthermia*, 10 (1994), 4, pp. 457-483
- [14] Damianou, C. A., Hynynen, K, Fan, X., Evaluation of Accuracy of a Theoretical Model for Predicting the Necroses Tissue Volume during Focused Ultrasound Surgery, *IEEE Trans. Ultrason. Ferroelect. Freq. Contr.*, 42 (1995), 2, pp. 182-187
- [15] Gowrishankar, T. R., *et al.*, Transport Lattice Models of Heat Transport in Skin with Spatially Heterogeneous Temperature-Dependent Perfusion, *Biomedical Engineering Online*, 3 (2004), article 42
<http://www.pubmedcentral.nih.gov/articlerender.fcgi?artid=544831>
- [16] Brown, S. L., Hunt, J. W, Hill, R. P., Differential Thermal Sensitivity of Tumor and Normal Micro-Vascular Response during Hyperthermia, *Int. J. Hyperth.*, 8 (1992), 4, pp. 501-514